Floer homology and the Homfly polynomial

Tamás Kálmán (Tokyo Institute of Technology)*

Abstract

We survey a set of results which establish a new connection between Floer homology groups of three-manifolds and quantum invariants of knots. They provide a way of computing certain coefficients of the Homfly polynomial of a special alternating link from the Floer homology of a sutured manifold that is closely related to the branched double cover of the link. The work has a strong discrete mathematical component: We identify the supporting set of spin^c structures of Floer homology with the set of hypertrees of a hypergraph, and define a version of the Tutte polynomial for the hypergraph.

1. Introduction

Low-dimensional topology of the past 20 years was dominated by two discoveries. One is that holomorphic curve-counting techniques can be used to associate Floer homology groups to compact three-dimensional manifolds and that these groups reflect geometric properties of the manifolds in some profound ways. There are three main versions of this construction (Seiberg–Witten, Heegaard–Floer, and embedded contact homology) and they are known to be equivalent. We will use the terminology of the Heegaard–Floer version, due to Ozsváth and Szabó, with the significant addition of sutured Floer homology by Juhász.

The other breakthrough that occurred around 2000 is the categorification of quantum knot invariants, in particular the Jones and Homfly polynomials, into homology theories called Khovanov homology and Khovanov–Rozansky homology, respectively, after their discoverers. These are essentially algebraic constructions, relying on recent advances in representation theory. They provide even more powerful knot invariants than their Euler characteristics but they also deepen the mystery of those knot polynomials. Indeed, we lack a satisfactory geometric interpretation of these homology groups, or in most cases even the accompanying polynomials.

There persists a hope that the missing geometric insight may come from Floer theory. There are deep structural similarities between the two kinds of homology groups (see [3]), yet to date the closest connection that was found between them is a spectral sequence that starts from a version of Khovanov homology of a knot and converges to the Floer homology of the branched double cover of the knot [17].

The connection that we are about to explain proceeds the other way, from Floer homology to quantum invariants. It only concerns the Homfly polynomial and not its categorification, and it only applies to certain 'nice' knots; in fact even then, only to some coefficients in their polynomials. (To be precise, we will look at special alternating links; via the Murasugi star product operation [14], our results extend to homogeneous

The author was supported by a Japan Society for the Promotion of Science (JSPS) Grant-in-Aid for Scientific Research C (no. 17K05244).

Keywords: sutured Floer homology, Alexander polynomial, Homfly polynomial, Seifert surface, branched double cover, special diagram, special alternating link, homogeneous link, bipartite graph, hypergraph, hypertree, root polytope, Tutte polynomial, interior polynomial.

* e-mail: kalman@math.titech.ac.jp
web: www.math.titech.ac.jp/~kalman

links, which include all alternating and all positive links.) So perhaps the work here is best viewed as a case study which, hopefully, hints at the existence of a larger picture. Having said that, we will in fact start with presenting results which do apply to all knots, but only go as far as their Alexander polynomials; then we will make an additional assumption that allows us access to the Homfly polynomial.

On the other hand, the formulas that we obtain for our Homfly coefficients are concrete and computable, moreover they make a very direct use of the geometric situation. The main ingredient in them, the so called interior polynomial [7] of a hypergraph, is a new discovery that has garnered independent interest in its own right [9, 12, 10, 16]. Interior polynomials may be associated to integer polymatroids, also known as finite M-convex sets. In fact, by now there exists a two-variable version of this polynomial that provides a full generalization of the Tutte polynomial of a matroid to polymatroids [2, 1]. All this grew out of an investigation of the Homfly polynomials of relatively simple knots. We believe this to be an indication that there is plenty of unexplored richness left in quantum invariants, as well as in Floer homology.

As to the project presented here, as we will see, a natural next step is to extend the interior polynomial to signed bipartite graphs. This has already been done by K. Kato [11], who also connected his notion to the Homfly polynomial. Research is ongoing on the Floer homology side of the picture.

2. Sutured manifolds from special diagrams

We will consider knot and link diagrams in the two-dimensional sphere S^2. As a warm-up, recall that every oriented link has a *special diagram*, that is a diagram in which no Seifert circle separates other Seifert circles from each other. A special diagram is the opposite of a braid diagram, and just like a braid, it is highly non-unique. Figure 1 shows a standard diagram of the Kinoshita–Terasaka knot, which is not special, and a deformation of it that results in a special diagram.

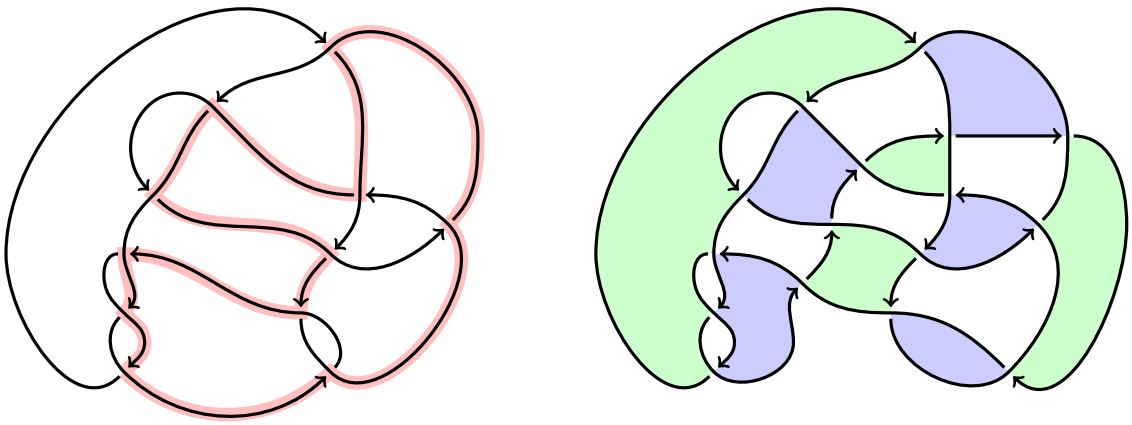

Figure 1: Left: a non-special diagram of the Kinoshita–Terasaka knot (with its type II Seifert circle highlighted). Right: a special diagram of the same knot with the interiors of its Seifert circles (now all type I) shaded.

Connected special diagrams are such that with respect to their checkerboard coloring, the boundaries of the regions of one of the two colors coincide with the Seifert circles of the diagram. These regions are divided into two classes E and V according

to the orientation (clockwise for E, counterclockwise for V) of their boundary. See the right side of Figure 1 for an example. Thus for a special diagram, its Seifert graph G is not only bipartite (which is always true) but it also comes with a natural embedding in S^2. We illustrate this in Figure 2. Note also that the edges of G inherit the sign of the corresponding crossing of the diagram. We indicate this by drawing positive edges solid and negative edges dotted.

Conversely, if G is a *connected, signed plane bipartite graph* with color classes E and V, then it gives rise to a special link diagram by the median construction. We will denote the corresponding link type by L_G. (Also, L_G has an obvious Seifert surface F_G that deformation retracts onto G; Figure 2 shows an example.) From now on we will treat G as our central object but our goal will remain to study the invariants of L_G.

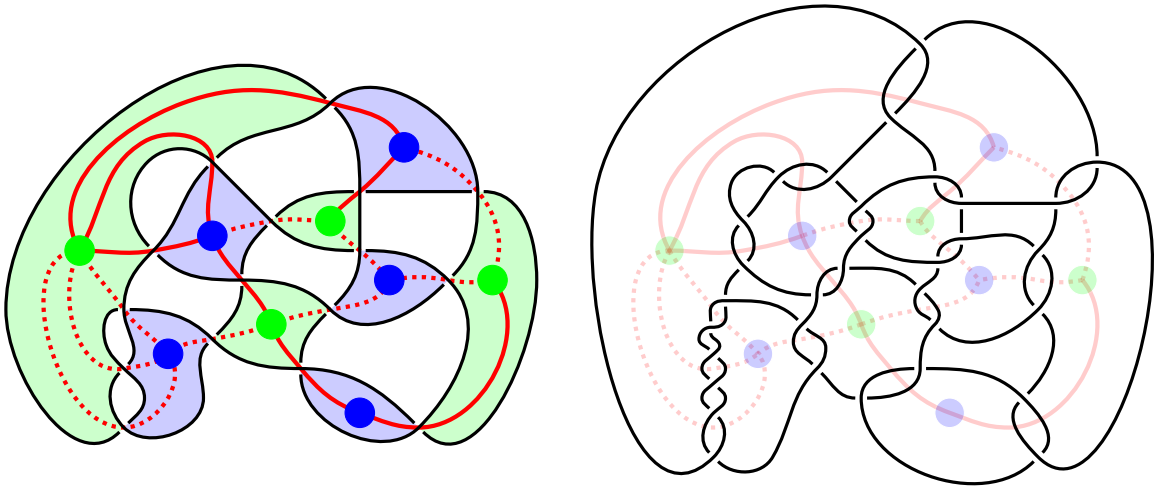

Figure 2: Left: the Seifert graph G of our special diagram L_G. Right: the link diagram $\tilde{L}_G$ obtained by doubling each crossing of L_G. The new link is a union of unknots.

Next, let us use Figure 3 to define a simple diagrammatic operation which we call *doubling*. When we carry this out at every crossing of our diagram of L_G (see Figure 2 for an example), the result is a diagram for a new link $\tilde{L}_G$ that consists of an unknot component for every vertex of G. We orient $\tilde{L}_G$ so that each of its components runs counterclockwise around the corresponding vertex. Then $\tilde{L}_G$ has an obvious Seifert surface $\tilde{F}_G$, an example of which is shown in Figure 4.

Figure 3: The doubling operation.

A central object in this research is the sutured manifold

$$\tilde{M}_G = (S^3 \setminus \tilde{F}_G, \tilde{L}_G),$$

obtained by cutting open the ambient manifold S^3 along $\tilde{F}_G$. This is a handlebody constructed from two three-balls (the inside and outside of S^2) with a one-handle connecting them for each vertex of G, that is, for each element of $E \cup V$. What might make it an interesting space is the suture $\tilde{L}_G$. This, too, has its components labeled by $E \cup V$ but a suture component indexed by a vertex does not only run along the handle indexed by the same vertex (which it may do several times, with zero times being a possibility); it also runs once along each handle indexed by an adjacent vertex.

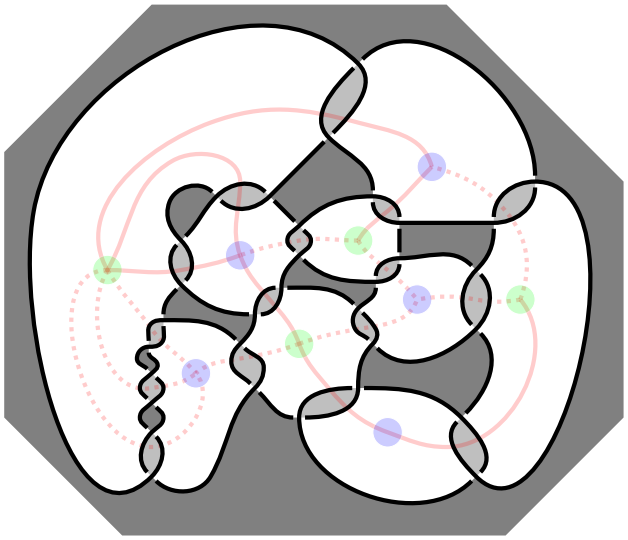

Figure 4: A Seifert surface $\tilde{F}_G$ of the doubled link $\tilde{L}_G$. The 'unbounded region' is in fact a disk region in S^2. The complement of the surface is the handlebody $\tilde{M}_G$.

We consider the sutured Floer homology group $\mathrm{SFH}(\tilde{M}_G)$. Recall that it has a direct sum decomposition with terms indexed by so called spin^c structures. Hence its Euler characteristic is naturally a function

$$\chi = \chi_{\tilde{M}_G} \colon \mathrm{Spin}^c(\tilde{M}_G) \to \mathbf{Z},$$

where $\mathrm{Spin}^c(\tilde{M}_G)$ is an affine space over the free Abelian group $H_1(\tilde{M}_G)$. The latter can be thought of as a corank 1 subgroup of $\mathbf{Z}^E \oplus \mathbf{Z}^V$; in particular, the linear functional

$$\alpha = \text{sum of the } V\text{-coordinates}$$

is well-defined over it. (This just measures how many times, algebraically, a 1-cycle runs over handles indexed by elements of V.) Hence, up to an additive constant, α is well-defined over $\mathrm{Spin}^c(\tilde{M}_G)$. With D. Thurston, we made the following observation.

Proposition 2.1. *The sequence of sums of χ-values along consecutive level sets of α, up to an overall sign, agrees with the coefficient sequence of $\Delta_{L_G}(-t)$, where Δ_{L_G} is the Alexander polynomial of L_G.*

Note that while $\mathrm{SFH}(\tilde{M}_G)$ may not be readily computable, its Euler characteristic χ is, by the 'decategorification' due to Friedl, Juhász, and Rasmussen [4].

In our example of Figure 4, we find 77 spin^c structures (in an 8-dimensional integer lattice) with $\chi \neq 0$. Among them, 39 have $\chi = 1$ and 38 have $\chi = -1$. These χ-values sum to 0 along all but one level set of α, reflecting the fact that the Alexander polynomial of the Kinoshita–Terasaka knot is 1.

Conjecture 2.2. *For our class of sutured manifolds $\tilde{M}_G$, the Euler characteristic χ only takes values 0 and ± 1. (There is a more concrete form which we omit here.)*

Returning to the topology of $\tilde{M}_G$ and the observation that its suture $\tilde{L}_G$ has many unknot components, we find the following claim. One might hope that this indicates a deeper relationship between our results and Ozsváth–Szabó's spectral sequence.

Proposition 2.3. *Let us extend $\tilde{M}_G$ by attaching a two-handle to each component of $\tilde{L}_G$, as well as two three-balls to the resulting boundary components. The closed three-manifold thus obtained is the branched double cover $\tilde{S}^3_{L_G}$ of S^3 along L_G.*

Corollary 2.4. *There is a Heegaard diagram for $\tilde{S}^3_{L_G}$ (and thus a Heegaard Floer chain complex for $\widehat{\mathrm{HF}}(\tilde{S}^3_{L_G})$) so that a Heegaard Floer chain complex for $\mathrm{SFH}(\tilde{M}_G)$ can be obtained from it by adding a new 'base point' for each vertex of G.*

This concludes our list of the properties of $\tilde{M}_G$ that hold for all special diagrams, i.e., for all oriented links. We note that Proposition 2.1 nay not be entirely surprising, given the well known relationship between the Alexander polynomial and Floer homology. In the next section we go beyond Δ_{L_G}, but that requires an extra assumption.

3. Special alternating links and Homfly polynomials

From now on we assume that all signs in G are positive. Then L_G, as well as $\tilde{L}_G$, is a (positive) special alternating link. (See Figure 5 for an example.) The sutured manifold $\tilde{M}_G$ is a so called L-space (see [4] for details), which implies that $\chi_{\tilde{M}_G}$ only takes the values 0 and 1; furthermore, for each spin^c structure $s \in \mathrm{Spin}^c(\tilde{M}_G)$, having $\chi(s) = 0$ implies $\mathrm{SFH}(\tilde{M}_G; s) = 0$ and

$$\chi(s) = 1 \text{ implies } \mathrm{SFH}(\tilde{M}_G; s) \cong \mathbf{Z}.$$

Let us call the latter set of spin^c structures the *support* of $\mathrm{SFH}(\tilde{M}_G)$.

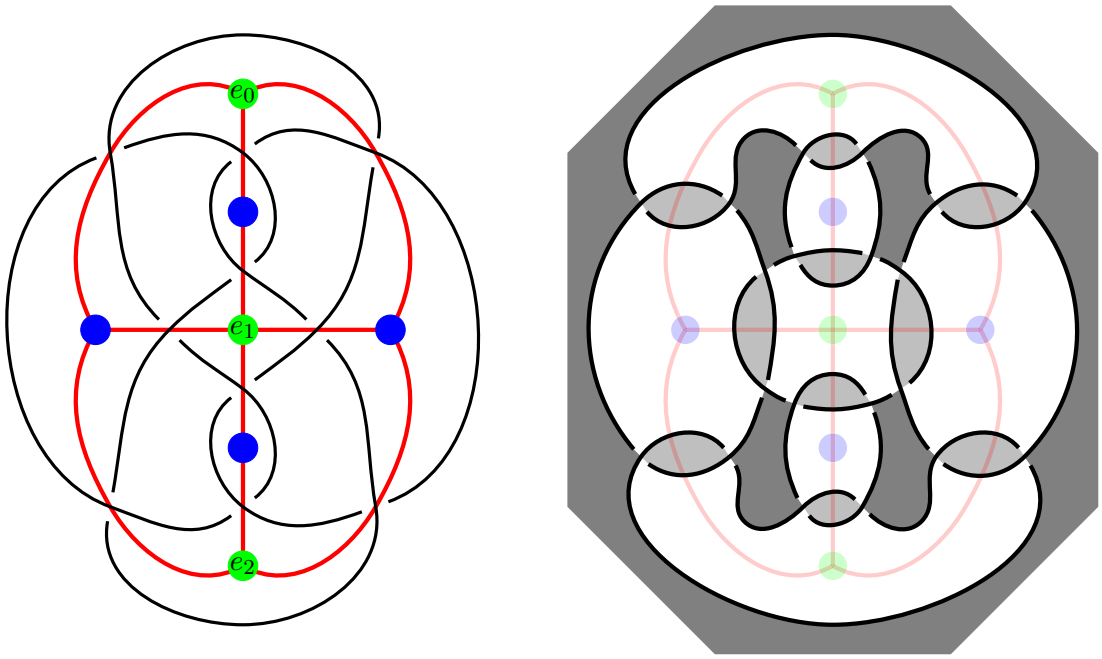

Figure 5: Left: a plane bipartite graph G and the corresponding special alternating knot L_G. Right: The surface $\tilde{F}_G$ whose complement $\tilde{M}_G$ we associate to the knot.

We will focus on the leading coefficient of the Alexander polynomial Δ_{L_G} and the corresponding terms in the Homfly polynomial P_{L_G}. Here $P = P(v,t)$ is defined by the initial condition $P_{\text{unknot}} = 1$ and the skein relation

$$v^{-1}P_{\nearrow} - v\,P_{\nearrow} = (t^{1/2} - t^{-1/2})P_{\sim},$$

and it reduces to Δ by setting $v = 1$. The *top* of P is the coefficient of $t^{b_1(G)/2}$ in P, where one-half of the first Betti number of G is Morton's upper bound [13] on the t-degree of P. This is known to be sharp in our class of cases. For example, the knot L_G of Figure 5 (found as 10_{120} in Rolfsen's table) has the Homfly polynomial

$$P_{L_G}(v,t) = \begin{array}{rrrrr} v^4t^2 & +4v^6t^2 & +3v^8t^2 & & \\ -4v^4t & -9v^6t & -9v^8t & -4v^{10}t & \\ +6v^4 & +13v^6 & +12v^8 & +5v^{10} & +v^{12} \\ -4v^4t^{-1} & -9v^6t^{-1} & -9v^8t^{-1} & -4v^{10}t^{-1} & \\ v^4t^{-2} & +4v^6t^{-2} & +3v^8t^{-2}; & & \end{array}$$

that is, in this case the leading coefficient of Δ_{L_G} is 8, which is partitioned by P_{L_G} as $8 = 1 + 4 + 3$. More precisely, the top of P is $v^4(1 + 4v^2 + 3v^4)$. Note that $b_1(G) = 4$.

To isolate the spin^c structures of $\tilde{M}_G$ (in the support of $\mathrm{SFH}(\tilde{M}_G)$) where α takes its maximum, we cut all those handles of $\tilde{M}_G$ that correspond to elements of V, by the obvious disks (of the correct co-orientation). This is done in the sense of surface decompositions of sutured manifolds; see [5] for details. The local operation is shown in Figure 6. As to the global picture, we realized the following in joint work with Juhász.

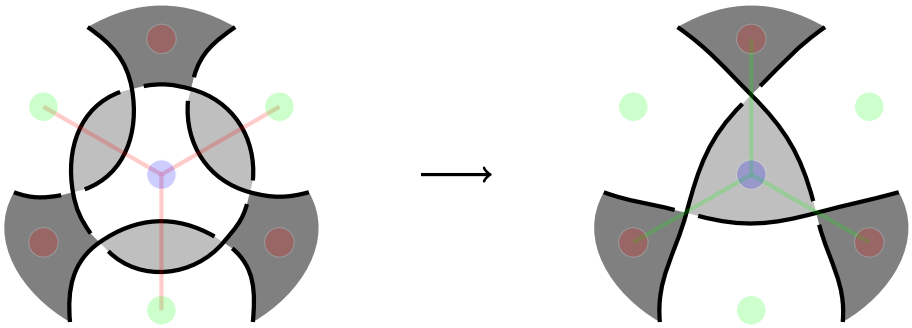

Figure 6: The effect of cutting a one-handle of $\tilde{M}_G$ along its co-core disk. On the right, the (faint) edges belong to the derived graph G_E, the curved arcs are part of the new special alternating link L_{G_E}, and the shaded regions represent its Seifert surface F_{G_E}.

Proposition 3.1. *After cutting all one-handles of $\tilde{M}_G$ that are indexed by an element of V, we obtain the sutured manifold*

$$M_{G_E} = \left(S^3 \setminus F_{G_E}, L_{G_E}\right).$$

Here the plane bipartite graph G_E is derived from G by placing a vertex in each region of G and connecting it to all elements of V that are incident with the region. The special alternating link L_{G_E} and its canonical Seifert surface F_{G_E} are associated to G_E by the median construction.

The set of points that mark the regions of G will be denoted by R. From the graph theory point of view, the roles of the sets E, V, and R are perfectly symmetric: they

all become vertices in a structure, called a *trinity*, that was first studied by Tutte. In particular, the original graph G may be renamed as G_R and there is also a third plane bipartite graph G_V. See [7] for details.

The following statement follows as a special case from the main result of [6], joint with Juhász and Rasmussen.

Theorem 3.2. *Those elements of the support of* $\mathrm{SFH}(\tilde{M}_G)$ *where* α *takes its maximum, which is affine equivalent to the support of* $\mathrm{SFH}(M_{G_E})$*, is also affine equivalent to the set of vectors*

$$B_{(V,E)} = \left\{ \mathbf{f}\colon E \to \mathbf{Z}_{\geq 0} \;\middle|\; \begin{array}{l} \text{there exists a spanning tree of } G \\ \text{with degree } \mathbf{f}(e)+1 \text{ at each } e \in E \end{array} \right\} \subset \mathbf{Z}^E.$$

Note that this description takes us back to our original graph G. The symmetry between its color classes E and V is (temporarily) broken. The elements of $B_{(V,E)}$ are called *hypertrees* in G, more precisely in the hypergraph with vertex set V and hyperedge set E; this explains our unusual choice of symbols. Let us also mention that $B_{(V,E)}$ is the set of lattice points in a convex polytope. See Figure 7 for an example and [7] for details.

Now, we may summarize some joint results with H. Murakami [8] and Postnikov [9], along with an observation of Kato [11], as follows. (We skip the explanation of the middle two items. See [15, 18] for an introduction.)

The top of the Homfly polynomial P_{L_G}

$\sim$ the h-vector of an arbitrary triangulation of the root polytope of G

$\sim$ the Ehrhart h^*-vector of the root polytope

$\sim$ the interior polynomial of the hypergraph (V, E),

where $\sim$ means that all these polynomials are equivalent by trivial changes of the variables. In particular,

$$\text{the top of } P_{L_G} = v^{b_1(G)} \cdot I_{(V,E)}(v^2),$$

where I stands for the interior polynomial. We remark that this implies $I_{(V,E)} = I_{(E,V)}$ for any planar bipartite graph and the main result of [9] is that the same holds for all so called transpose pairs of hypergraphs.

4. Polynomial invariants of hypergraphs

We close this survey by a description of how $I_{(V,E)}$ is computed from $B_{(V,E)}$, as this (with the help of Theorem 3.2) is how Homfly coefficients can be derived from Floer homology. (There is also an exterior polynomial $X_{(V,E)}$ [7], and a common two-variable extension of I and X [2, 1], whose descriptions we omit.)

The *hypergraph* structure induced by G is nothing but the multiset of subsets of V, where each $e \in E$ is identified by the set of its neighbors. An easy observation is that for each hypertree $\mathbf{f} \in B_{(V,E)}$, the sum of its values is a constant, namely $\sum_{e \in E} \mathbf{f}(e) = |V| - 1$.

We fix an arbitrary total order on the set E, say $e_0 < e_1 < \cdots < e_k$. For each hypertree $\mathbf{f} \in B_{(V,E)}$, we count those hyperedges e_i for which there exists an index $0 \leq j < i$ so that by increasing the value of $\mathbf{f}$ by 1 at e_j and decreasing it by 1 at e_i, we obtain a new hypertree. These hyperedges are called *(internally) inactive* for $\mathbf{f}$ and their number $\bar{\iota}(\mathbf{f})$ is called the *internal inactivity* of $\mathbf{f}$.

The *interior polynomial* of our hypergraph is

$$I_{(V,E)}(\xi) = \sum_{\mathbf{f} \in B_{(V,E)}} \xi^{\bar{\iota}(\mathbf{f})}.$$

Remarkably, it does not depend on the order which we use to define $\bar{\iota}(\mathbf{f})$ [7], even though individual values of $\bar{\iota}$ are sensitive to changes in the order.

In our example of Figure 5, let us choose the three-element color class to play the role of hyperedges. We find 8 hypertrees, which are three-dimensional vectors arranged along a two-dimensional plane as shown in Figure 7. This can easily be verified by sketching some spanning trees of G.

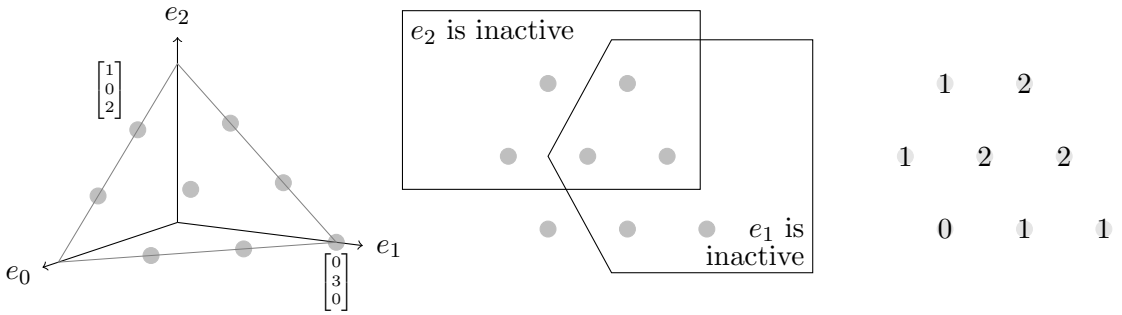

Figure 7: Hypertrees and their internal inactivities.

The least element e_0 of E is never inactive for any hypertree. To decide whether e_1 is inactive for a hypertree $\mathbf{f}$, we check whether there is a hypertree immediately to the left of $\mathbf{f}$. In Figure 7 we see that in five cases there is (e_1 is inactive) and in three cases there is not. Regarding e_2, the criterion is whether there is a hypertree below and to the left *or* below and to the right of $\mathbf{f}$. The answer is yes (e_2 is inactive) again in five cases, but it is not the same five. The data is collected at the right side of Figure 7: one hypertree has internal inactivity $\bar{\iota} = 0$, four have $\bar{\iota} = 1$, and three have $\bar{\iota} = 2$. Thus the interior polynomial has the coefficients 1, 4, and 3, exactly as we saw along the top of the Homfly polynomial.

References

[1] O. Bernardi, T. Kálmán, and A. Postnikov, *The universal Tutte polynomial*, in preparation.

[2] A. Cameron and A. Fink, *The Tutte polynomial via lattice point counting*, arXiv:1802.09859.

[3] N. Dunfield, S. Gukov, and J. Rasmussen, *The Superpolynomial for Knot Homologies*, Experimental Math. 15 (2006), 129–159.

[4] S. Friedl, A. Juhász, and J. Rasmussen, *The decategorification of sutured Floer homology*, J. Topol. 4 (2011), no. 2, 431–478.

[5] A. Juhász, *Floer homology and surface decompositions*, Geom. Topol. 12 (2008), 299–350.

[6] A. Juhász, T. Kálmán, and J. Rasmussen, *Sutured Floer homology and hypergraphs*, Math. Res. Lett. 19 (2012), no. 6, 1309–1328.

[7] T. Kálmán, *A version of Tutte's polynomial for hypergraphs*, Adv. Math. 244 (2013), no. 10, 823–873.

[8] T. Kálmán and H. Murakami, *Root polytopes, parking functions, and the HOMFLY polynomial*, Quantum Topol. 8 (2017), no. 2, 205–248.

[9] T. Kálmán and A. Postnikov, *Root polytopes, Tutte polynomials, and a duality theorem for bipartite graphs*, Proc. London Math. Soc. 114 (2017), no. 3, 561–588.

[10] T. Kálmán and L. Tóthmérész, *Hypergraph polynomials and the Bernardi process*, arXiv:1810.00812.

[11] K. Kato, *Interior polynomial for signed bipartite graphs and the HOMFLY polynomial*, arXiv:1705.05063.

[12] K. Kato, *A mirroring formula for the interior polynomial of a bipartite graph*, arXiv:1804.09952.

[13] H. Morton, *Seifert circles and knot polynomials*, Math. Proc. Camb. Phil. Soc. 99 (1986), 107–109.

[14] K. Murasugi and J. Przytycki, *The skein polynomial of a planar star product of two links*, Math. Proc. Camb. Phil. Soc. 106 (1989), 273–276.

[15] H. Ohsugi and T. Hibi, *Normal polytopes arising from finite graphs*, J. Algebra 207 (1998), no. 2, 409–426.

[16] H. Ohsugi and A. Tsuchiya, *Reflexive polytopes arising from bipartite graphs with γ-positivity associated to interior polynomials*, arXiv:1810.12258.

[17] P. Ozsváth and Z. Szabó, *On the Heegaard Floer homology of branched double-covers*, Adv. Math. 194 (2005), no. 1, 1–33.

[18] A. Postnikov, *Permutohedra, Associahedra, and Beyond*, Int. Math. Res. Not. 2009, no. 6, 1026–1106.